Ionics (2015) 21:1781–1786
DOI 10.1007/s11581-014-1316-8

ORIGINAL PAPER

Nanostructured photoelectrochemical solar cells with polyaniline nanobelts acting as hole conductors

Xiaoping Zhang · Zhang Lan · Shuohui Cao · Jiangli Wang · Zhong Chen

Received: 10 June 2014 / Revised: 20 October 2014 / Accepted: 12 November 2014 / Published online: 25 November 2014

Abstract Nanostructured photoelectrochemical solar cells have been prepared by combining a Sb_2S_3-sensitized photoactive electrode, polyaniline nanobelts, and a Ag counter electrode to form a layered structure. Here, Sb_2S_3 acts as an absorbing semiconductor, and polyaniline acts as both a hole conductor and light absorber (a hole-conducting dye). Via the optimization that eventually determines the chemical bath deposition duration to be 3 h, the cell shows a high photovoltaic performance with 7.05 mA/cm^2-short-circuit current density, 0.695 V-open-circuit voltage, 0.457 fill factor, and 2.24 % power conversion efficiency. The prepared devices are stable under room light in ambient conditions (even without encapsulation).

Keywords Sb_2S_3-sensitized · Polyaniline · Ag counter electrode · Photoelectrochemical solar cell

Introduction

Sunlight is an abundant and renewable energy resource. Converting sunlight into electricity has been regarded as one of the most promising approaches to provide clean energy. Conventional solar cells, such as silicon solar cells, have been widely researched in recent years, and quantum confined inorganic semiconductors have attracted extensive attention and research interests [1–4]. Among the quantum dot solar cells, Sb_2S_3 (stibnite) is a promising semiconductor sensitizer due to its relative abundance in the earth's crust, high absorption coefficient (1.8×10^5 cm^{-1} at 450 nm), and a mid-range optical bandgap of 1.7–1.8 eV, which is well suitable for capturing visible light photons [5, 6]. Both solid and liquid junctions of Sb_2S_3-sensitized photoelectrochemical solar cells have been reported [7, 8], where Sb_2S_3 is usually deposited by the chemical bath deposition (CBD) method. Stibnite has been studied previously as a potential sensitizer for TiO_2 photoanode in photoelectrochemical solar cell employing sulfide liquid electrolyte [9]. A solar cell using crystalline Sb_2S_3 deposited on flat TiO_2 was investigated [10], with its power conversion efficiency as low as 0.001 %. However, it has been found that the Sb_2S_3-sensitized photoanode is instable in sulfide liquid electrolyte. Recently, to overcome this disadvantage, solid-state organic hole-transporting materials of spiro-MeOTAD [2,22′,7,77′-tetrkis (*N*,*N*-di-*p*-methoxyphenylamine)-9,99′-spirobi fluorine] have been investigated, yielding a 5 % conversion efficiency. Another Sb_2S_3-sensitized solid-state solar cell with poly (3-hexylthiophene) (P_3HT) as both a hole conductor and a light absorber (a hole-conducting dye) was prepared; the power conversion efficiency as high as 5.13 % has recently been achieved [11]. Furthermore, inorganic p-type materials, such as CuI [12] and CuSCN [13], conducting polymers such as poly (3,4-ethylenedioxythiophene) PEDOT [14], polyaniline [15], polydiacetylene [16], and so forth have also been studied as materials for fabricating solid hole transporters.

Here, we use polyaniline (PAn) nanobelts as the hole transporter to fabricate Sb_2S_3-sensitized solar cells. A high power conversion efficiency of the cell, 2.24 %, is obtained through optimizing the duration of chemical bath deposition (CBD) of Sb_2S_3 on the photoactive electrode. The proposed model (TiO_2/Sb_2S_3/PAn/Ag solar cell) shows high maneuverabilities, though the power conversion efficiency is a little

X. Zhang · S. Cao · J. Wang · Z. Chen (✉)
Department of Electronic Science, Fujian Provincial Key Laboratory of Plasma and Magnetic Resonance, State Key Laboratory for Physical Chemistry of Solid Surfaces, Xiamen University, Xiamen 361005, China
e-mail: chenz@xmu.edu.cn

Z. Lan
Institute of Materials Physical Chemistry, Huaqiao University, Xiamen 361021, China

lower than a recent $TiO_2/Sb_2S_3/P_3HT/Au$ solar cell [11], indicating the nano-PAn as a new promising material in solar cell research. In this report, the nanostructure and performances of polyaniline doped by hydrochloric acid is analyzed by UV–vis, scanning electronic microscope and infrared spectroscopy. Results demonstrate that the reaction of polyaniline doped by hydrochloric acid takes place in a quinine ring. The dope polyanilines exhibits the nanobelt structure and uniformity distribution, thus revealing a high electrical conductivity.

Experiments

Materials

Titanium isopropoxide, nitric acid, glacial acetic acid, acetone, poly (ethylene glycol) with average molecular weight 20,000, antimony (III) chloride, sodium thiosulfate pentahydrate, ammonium peroxydisulfate aniline, silver nitrate, N-vinyl pyrazole ketone of alkanes (PVP, K-30), ethanediol, and ferric chloride were all A. R. Grade and were purchased from Sinopharm Chemical Reagent Co., Ltd, China. All reagents were used without further treatments. Conducting glass plates (FTO glass, fluorine doped tin oxide over-layer, sheet resistance 15 $\Omega \cdot sq^{-1}$, purchased from Nippon Glass Co. JP) were used as substrates for precipitating TiO_2 films.

Preparation of Sb_2S_3-sensitized TiO_2 photoactive electrodes

Nanocrystal TiO_2 particles of approximately 10–20 nm were synthesized with the same method as reported in Ref. [17]. Nanocrystal TiO_2 particles (10 g), poly (ethylene glycol) (3 g), and de-ionized water (30 mL) were mixed and stirred on a hot plate to adjust to a suitable viscosity for preparing 10-μm-thick TiO_2 films on FTO glasses by the doctor-blade method. Then, titanium dioxide films were sintered at 450 °C for 0.5 h. Pre-prepared TiO_2 films were sensitized with Sb_2S_3 by chemical bath deposition (CBD) similar to the method described by Messina et al. [18, 19]. The difference lies in that the acetone solvent was substituted by glacial acetic acid. Sintered TiO_2 films were immersed into the mixture containing 5-mL glacial acetic acid and 45-mL aqueous solution with 0.05 M $SbCl_3$ and 0.05 M $Na_2S_2O_3$ at room temperature for different times. Samples were prepared with different deposition times ranging from 1 to 4 h, and were cleaned with de-ionized water to remove any sulfate or chloride residues, and were finally dried in a vacuum oven at 120 °C for 2 h.

Preparation of PAn nanobelts

Polyaniline nanobelts were prepared as follows: 1-mL aniline was first dissolved in 25-mL 1 M HCl aqueous solution. Then, another 25-mL 1 M HCl containing 0.85-g ammonium persulfate was added under vigorous stirring and was kept at room temperature for 1 h. The synthesized PAn was collected by centrifuging at 4000 rpm and was cleaned with 1 M HCl aqueous solution and ethanol both three times. After this procedure, 0.5-g cleaned PAn was re-dispersed in 100-mL de-ionized water under vigorous stirring and ultrasound sonication to form homogeneous aqueous dispersion.

Preparation of Ag counter electrode

First, 10-mL 0.15 mol/L PVP glycol solution was prepared and stirred quickly. Then 10 mL of the solution was added to 10-mL 0.1 mol/L $AgNO_3$ glycol solution under vigorous stirring. The resultant solution was autoclaved at 165 °C for 2.5 h to form milky white slurry and kept at room temperature for 1 h. A large amount of acetone was added and ultrasonicated for 30 min. Finally, the silver nanoparticles were collected by centrifuging at 4000 rpm and were cleaned with ethanol once. Ultimately, the silver nanoparticles were stored in ethanol.

Assembling of TiO_2/Sb_2S_3/PAn/Ag solar cells

Nanostructured TiO_2/Sb_2S_3/PAn/Ag solar cells were assembled as follows. A drop of PAn nanobelts aqueous dispersion was dipped on the Sb_2S_3-sensitized TiO_2 photoactive electrode, and then the Ag nanoparticles solution was dumped on it. Next the sandwich type cell was placed on a hot plate at 60 °C to vaporize de-ionized water and ethanol. Finally, a cyanoacrylate adhesive was used as sealant to seal the device. Bisphenol A epoxy resin was used in a further sealing process.

Preparation of PAn film for FESEM images

PAn film is prepared as follows. First, the polyaniline aqueous dispersion is coated on FTO glass substrates by the doctor-blade method. Then, the PAn film was placed on a hot plate to vaporize de-ionized water.

Characterization

Morphologies of PAn nanobelts and silver nanoparticles were analyzed by a field emission scanning electron microscopy (FESEM) (S-4800, HITACHI) and a transmission electron microscopy (TEM) (H-7650, HITACHI). The UV–vis absorption was measured with a UV–vis 3100 spectrophotometer (Shimadzu, Japan). The infrared absorption (IR) was measured with a Nicolet Avatar 330 Fourier transform infrared spectrometer (Thermo Electron Corporation, USA). Photovoltaic tests were carried out by measuring J-V characteristic curves under simulated AM 1.5 G solar illumination at 100 $mW \cdot cm^{-2}$ from a xenon arc lamp (CHF-XM500, Trusttech Co, Ltd, China) in the ambient atmosphere and recorded with a CHI 660C electrochemical workstation. There

were 25 samples of solar cells; with five samples in each category, we tested five cells to measure their power conversion efficiency and took the average. To ensure that the characterization can be representative, we selected the cell that yielded a power conversion efficiency closest to this average value in each category as the typical sample. The active area of Sb_2S_3-sensitized solar cell was 0.12 cm^2 (0.3 × 0.4 cm^2).

Results and discussion

Morphologies of PAn material and PAn film are shown in Fig. 1. Figure 1a and b show FESEM images of the PAn film; Fig. 1c and d show TEM images of the polyaniline, which is dispersed in the water. It is seen that the synthesized PAn material exhibits the nanobelt structure. After the water vaporizes, a porous film is obtained. The well-connected network of PAn nanobelts in the film is beneficial for transporting holes. Morphologies of Ag counter electrode are shown in Fig. 2a and b. It is observed that the synthesized Ag catalyst shows nanoparticles structure. Because of small particle sizes and large specific surface areas, the Ag counter electrode shows higher catalytic activity. The TEM image (Fig. 2c) shows TiO_2 film is composed of nanoparticles and their boundaries could be clearly distinguished. After 3 h CBD of Sb_2S_3, the morphology of TiO_2 nanoparticles is changed; they are covered with a thin layer of Sb_2S_3, (Fig. 2d). This change provides an evidence that the TiO_2 film was successfully sensitized by a thin layer of Sb_2S_3. Ultimately, for the solar cells, owing to the maintained mesoporous morphology of the Sb_2S_3-photoactive electrode, the PAn hole conductor can partly penetrate into the photoactive electrode to form nanostructure as the traditional nanostructured photoelectrochemical solar cells.

Figure 3 shows UV–Vis absorption spectra of Sb_2S_3-sensitized TiO_2 films prepared with different CBD durations (0, 1, 2, 3, and 4 h) and PAn nanobelts. It is seen that Sb_2S_3-sensitized TiO_2 films can extend the light absorption edge to the visible wavelength region, but bare TiO_2 films (0 h) cannot, as shown in Fig. 3. Moreover, stibnite-sensitized TiO_2 films show the increased light absorbance with prolonging CBD durations. For example, after 3 h CBD duration, the Sb_2S_3-sensitized TiO_2 film exhibits a higher light absorbance in the wavelength region from 350 to 620 nm. For further increasing CBD durations, no conspicuous differences exist in the light absorbance among samples prepared with 3 and 4 h CBD duration. Apart from the changed light absorbance in the visible wavelength region, we can observe that Sb_2S_3-sensitized TiO_2 films can also increase the light absorbance in an ultraviolet wavelength interval between 250 and 400 nm. Hence, Sb_2S_3 is also an efficient sensitizer for absorbing ultraviolet light, as previously reported [20]. Additionally, after 3-h CBD duration, bare TiO_2 films are successfully sensitized by a thin layer of Sb_2S_3 [20]. Doped polyaniline

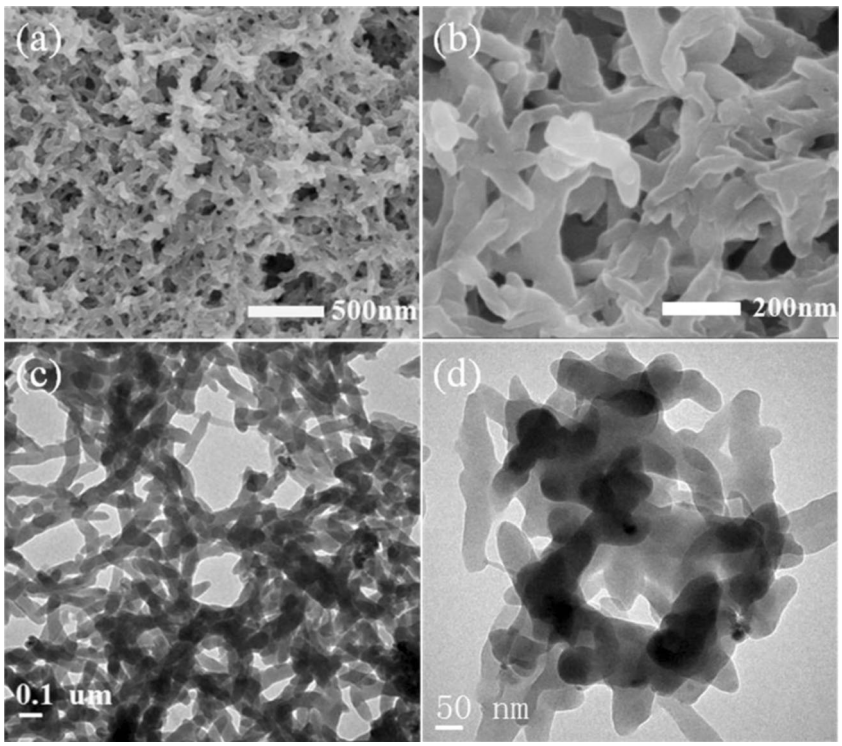

Fig. 1 FESEM images of the PAn film: **a** and **b** (**b** is the amplified localized image of **a**). TEM images of the PAn nanobelts: **c** and **d** (**d** is the amplified localized image of **c**)

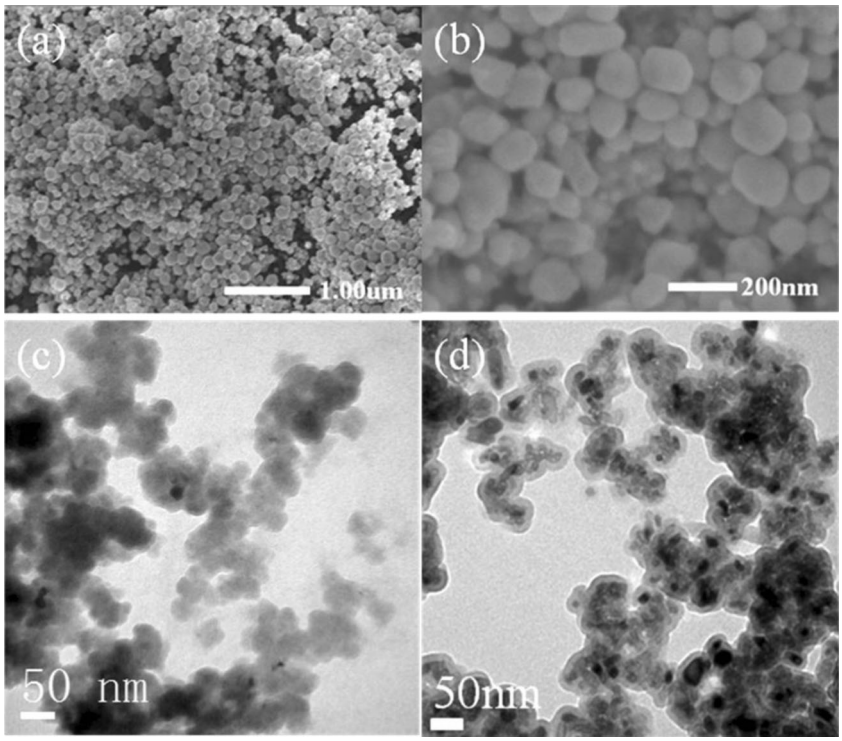

Fig. 2 FESEM images of the Ag nanoparticles counter electrode **a** and **b** (**b** is the amplified localized image of **a**). TEM images of the TiO_2 film (**c**) and Sb_2S_3-sensitized TiO_2 film (**d**) prepared with 3-h CBD duration

is a hole-conducting material that displays three absorption peaks in 350, 440, and 772 nm, respectively, as can be seen in Fig. 3 (PAn). The first is caused by the electron transition; the latter two are polaron peaks caused by doping. Because of the polaron peak, doped polyaniline can extend the edge of light absorption to the visible wavelength region.

Figure 4 shows the photovoltaic performance of Sb_2S_3-sensitized solar cells containing photoactive electrodes prepared with different CBD durations. Photovoltaic parameters, such as short-circuit current density (*Jsc*), open-circuit voltage (*Voc*), fill factor (*FF*), and power conversion efficiency (*Eff*) are listed in Table 1. From the data, we can find those values of *Jsc* increasing regularly with prolonging CBD duration for 3 h and then decreasing regularly by further increasing deposition times. This tendency of first increasing with prolonging CBD duration for 3 h is in conformity with the changed light absorbance of Sb_2S_3-sensitized TiO_2 films, as shown in Fig. 3. And then, the values of *Jsc* decreased; in the meantime, the increasing amplitude of the light absorbance is reduced. It is known that the light absorbance of photoactive electrodes in sensitized photoelectrochemical solar cells influences the power conversion ability of cells greatly [21]. As the case

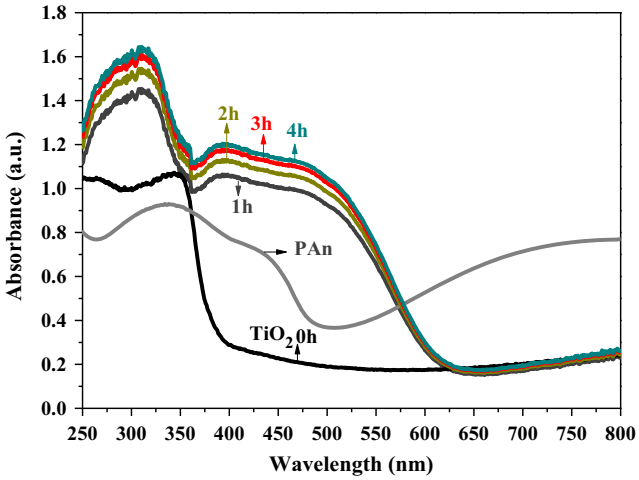

Fig. 3 UV–Vis absorption spectra of PAn nanobelts and the Sb_2S_3-sensitized TiO_2 films prepared with different CBD duration (0, 1, 2, 3, and 4 h)

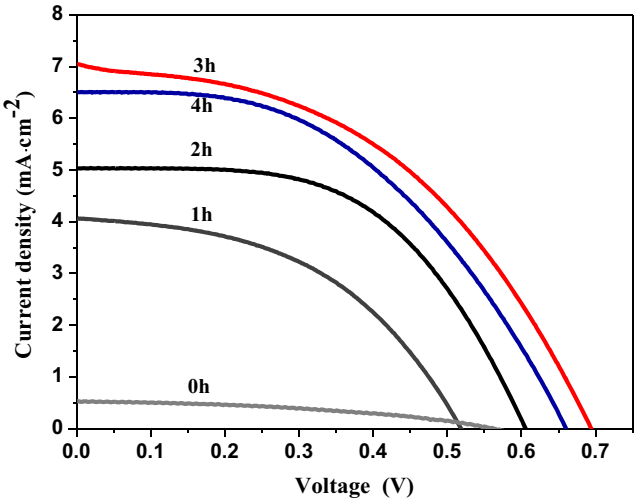

Fig. 4 Photocurrent-voltage curves of Sb_2S_3-sensitized solar cells containing photoactive electrodes prepared with different CBD durations

Table 1 Photovoltaic parameters of Sb_2S_3-sensitized solar cells shown in Fig. 4

Photoanode (h)	I_{sc} (mA·cm^{-2})	V_{oc} (V)	*FF*	*Eff* (%)
0	0.53	0.563	0.411	0.12
1	4.07	0.519	0.470	0.99
2	5.04	0.606	0.549	1.68
3	7.05	0.695	0.457	2.24
4	6.50	0.661	0.471	2.02

stands, the prolonging CBD duration can increase the coverage ratio of Sb_2S_3 thin layer on the TiO_2 surface by replenishing the uncovered area. Such increment of Sb_2S_3 loading leads to more excited electrons under the light, which is advantageous to generate the photocurrent in the Sb_2S_3-sensitized solar cell. However, as the thickness of the Sb_2S_3 layer increases with prolonging CBD duration, it will be more difficult to inject excited electrons generated in the outer layer into the TiO_2 matrix. It is also inferred layer that the Sb_2S_3/electrolyte contacting area will decrease with prolonging CBD duration because more pores are probably blocked by the additional loading of Sb_2S_3 [22].

We also observe the enhancement in *Voc* with an increase in the deposition time up to 3 h and then a negligible change in *Voc* with the deposition time from 3 to 4 h. The best cell exhibits *Jsc*, *Voc*, and *FF* values of 7.05 mA·cm^{-2}, 0.695 V, and 0.457, respectively, yielding a power conversion efficiency (*Eff*) of 2.24 %. The power conversion ability of solar cells without any sensitizers (0.12 %) is lower than that of Sb_2S_3-sensitized solar cells (2.24 %). At this juncture, we hypothesize that the better performance of proposed devices is due to the intimate contact between Sb_2S_3 and the PAn as suggested in Refs. [20, 23]. We have measured the UV–Vis absorption

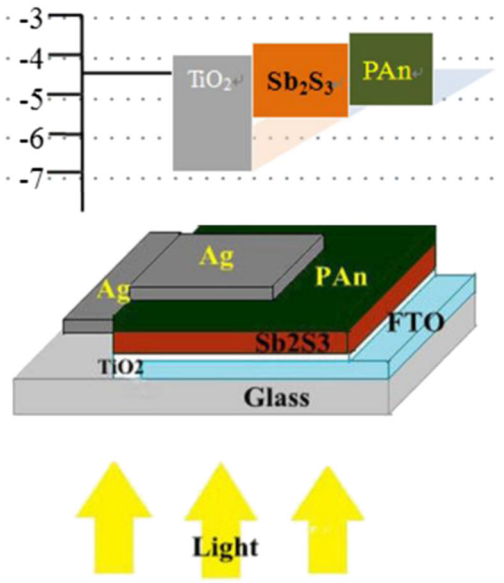

Fig. 5 The energy band diagram of the Sb_2S_3-sensitized solar cells

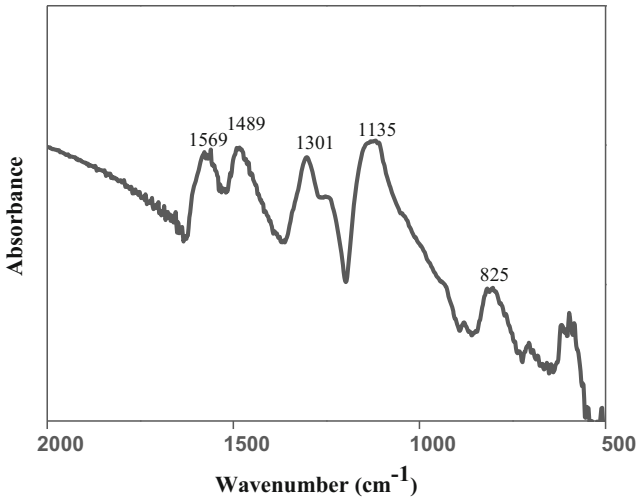

Fig. 6 The FT-IR spectrogram of polyaniline doped by hydrochloric acid

and cyclic voltammogram of PAn solution in order to obtain the highest occupied molecular orbital (HOMO) and the lowest unoccupied molecular orbital (LUMO) energy levels. The absorption edge of the PAn solution is located at 871 nm, so the band gap about 1.42 eV can be estimated with the equation of Eg=hc/λabs=1240/λabs [24]. The oxidation potential for the PAn solution can be obtained via cyclic voltammetry; then the HOMO is deduced by comparing to the energy level of ferrocene/ferrocenium (Fc/Fc+) to be 4.8 eV [25]. The oxidation potential about 0.33 eV vs Fc/Fc+ was obtained, so the HOMO about −5.13 eV can be calculated with the equation of HOMO=−[Eox−E(Fc/Fc+)+4.8]. The LUMO about −3.71 eV was obtained as the sum of the band gap and the HOMO. The energy band diagram of the Sb_2S_3-sensitized solar cells can be drawn, as shown in Fig. 5. It is known that energy bands among nanocrystal TiO_2 film, Sb_2S_3 sensitizer, and Ag are suitable for transporting light-induced charges. In other words, HOMO and LUMO levels in PAn are compatible with the conduction band of the Sb_2S_3 sensitizer and those in TiO_2 to drive the charge-transfer process.

Figure 6 shows the FT-IR spectrogram of polyaniline doped by hydrochloric acid. Ascriptions of peaks value are listed in Table 2. From the data, we can find that most significant changes of doped polyaniline are the C-C vibration in N=Q=N from 1600 to 1569 cm^{-1}. The value of the quinine ring shows a larger shift to low frequencies; the value of the

Table 2 Ascription of peak value show in Fig. 6

Peak value (cm^{-1})	Ascription
825	C-H vibration
1135	C-N vibration in N=Q=N
1301	C-N vibration in N-B-N
1489	C-C vibration in N-B-N
1569	C-C vibration in N=Q=N

benzene ring remains unchanged. We can find the reaction of polyaniline doped by hydrochloric acid taking place in the quinine ring. Thus, the dope polyaniline reveals a high redox reaction activity and high electrical conductivity, yielding a high power conversion efficiency.

Conclusions

Nanostructured photoelectrochemical solar cells are prepared by combining a Sb_2S_3-sensitized photoactive electrode, polyaniline nanobelts, and a Ag counter electrode to form a sandwiched structure. The highest power conversion efficiency of the cells, 2.24 %, was obtained by optimizing the CBD duration to become 3 h on the photoactive electrode. Polyanilines investigated in this study appear as a promising material to be used as the hole transporter in photoelectrochemical solar cells.

Acknowledgments This work was supported by the NNSF of China under grant 21327001.

References

1. He Z, Zhong C, Su S et al (2012) Enhanced power-conversion efficiency in polymer solar cells using an inverted device structure. Nat Photonics 6:591–595
2. Semonin OE, Luther JM, Choi S et al (2011) Peak external photocurrent quantum efficiency exceeding 100 % via MEG in a quantum dot solar cell. Science 334:1530–1533
3. Patel R, Ahn SH, Chi WS et al (2012) Poly (vinyl chloride)-graft-poly (N-vinyl caprolactam) graft copolymer: synthesis and use as template for porous TiO_2 thin films in dye-sensitized solar cells. Ionics 18:395–402
4. Dou L, You J, Yang J et al (2012) Tandem polymer solar cells featuring a spectrally matched low-bandgap polymer. Nat Photonics 6:180–185
5. Nishioka K, Sueto T, Saito N (2009) Formation of antireflection nanostructure for silicon solar cells using catalysis of single nano-sized silver particle. Appl Surf Sci 255:9504–9507
6. Itzhaik Y, Niitsoo O, Page M et al (2009) Sb_2S_3-sensitized nanoporous TiO_2 solar cells. J Phys Chem C 113:4254–4256
7. Boix PP, Larramona G, Jacob A et al (2011) Hole transport and recombination in all-solid Sb_2S_3-sensitized TiO_2 solar cells using CuSCN as hole transporter. J Phys Chem C 116:1579–1587
8. Savadogo O, Mandal KC (1993) Low-cost technique for preparing n-Sb_2S_3/p-Si heterojunction solar cells. Appl Phys Lett 63:228–230
9. Vogel R, Hoyer P, Weller H (1994) Quantum-sized PbS, CdS, Ag_2S, Sb_2S_3, and Bi_2S_3 particles as sensitizers for various nanoporous wide-bandgap semiconductors. J Phys Chem 98:3183–3188
10. Itzhaik Y, Niitsoo O, Page M et al (2009) Sb_2S_3-sensitized nanoporous TiO_2 solar cells. J Phys Chem C 113:4254–4256
11. Chang JA, Rhee JH, Im SH, Lee YH, Kim HJ, Seok SI, Gratzel M (2010) High-performance nanostructured inorganic–organic heterojunction solar cells. Nano Lett 10(7):2609–2612
12. Sirimanne PM, Tributsch H (2004) Parameters determining efficiency and degradation of TiO_2/dye/CuI solar cells. J Solid State Chem 177:1789–1795
13. Nanu M, Schoonman J, Goossens A (2004) Inorganic nanocomposites of n-and p-type semiconductors: a new type of three-dimensional solar cell. Adv Mater 16:453–456
14. Xia J, Masaki N, Lira-Cantu M et al (2008) Influence of doped anions on poly (3, 4-ethylenedioxythiophene) as hole conductors for iodine-free solid-state dye-sensitized solar cells. J Am Chem Soc 130:1258–1263
15. Tan SX, Zhai J, Wan MX et al (2003) Polyaniline as a hole transport material to prepare solid solar cells. Synth Met 137:1511–1512
16. You X, Zou G, Ye Q et al (2008) Ruthenium (II) complex-sensitized solid-state polymerization of diacetylene in the visible light region. J Mater Chem 18(39):4704–4711
17. Lan Z, Wu J, Lin J et al (2010) Dye-sensitized solar cell with a solid state organic–inorganic composite electrolyte containing catalytic functional polypyrrole nanoparticles. J Sol-Gel Sci Technol 53(3): 599–604
18. Messina S, Nair MTS, Nair PK (2007) Antimony sulfide thin films in chemically deposited thin film photovoltaic cells. Thin Solid Films 515:5777–5782
19. Messina S, Nair MTS, Nair PK (2009) Solar cells with Sb_2S_3 absorber films. Thin Solid Films 517:2503–2507
20. Lan Z, Zhang X, Wu J et al (2013) A novel photoelectrochemical solar cell with high efficiency in converting ultraviolet light to electricity. Electrochim Acta 108:337–342
21. Kongkanand A, Tvrdy K, Takechi K et al (2008) Quantum dot solar cells. Tuning photoresponse through size and shape control of CdSe-TiO_2 architecture. J Am Chem Soc 130:4007–4015
22. Hetsch F, Xu X, Wang H, Kershaw SV, Rogach AL (2011) Semiconductor nanocrystal quantum dots as solar cell components and photosensitizers: material, charge transfer, and separation aspects of some device topologies. J Phys Chem Lett 2(15):1879–1887
23. Xiaoping Z, Zhang L, Jihuai W et al (2013) Enhancing photovoltaic performance of photoelectrochemical solar cells with nano-sized ultra thin Sb_2S_3-sensitized layers in photoactive electrodes. J Mater Sci Mater Med 24(6):1970–1975
24. Pommerehne J, Vestweber H, Guss W et al (1995) Efficient two layer leds on a polymer blend basis. Adv Mater 7(6):551–554
25. Ganteför G, Gausa M, Meiwes-Broer KH et al (1990) Photoelectron spectroscopy of silver and palladium cluster anions. Electron delocalization versus, localization. J Chem Soc Faraday Trans 86(13): 2483–2488